united nations
educational, scientific
and cultural
organization

international atomic
energy agency

the
abdus salam
international centre for theoretical physics

H4.SMR/1304-6

"COLLEGE ON SOIL PHYSICS"

12 March - 6 April 2001

Soil Porous Systems: Models and Reality

M. Kutilek and D. R. Nielsen

Elsevier
Soil and Tillage Research (Journal)
Prague
Czech Republic

College on Soil Physics
ICTP, TRIESTE, 12-29 March, 2001

LECTURE NOTES

Soil Porous Systems: Models and Reality

Extended text of the textbook
Soil Hydrology, 1994 by M. Kutílek and D.R. Nielsen

Miroslav Kutílek

Professor Emeritus
Nad Patankou 34, 160 00 Prague 6, Czech Republic
Fax/Tel. +420 2 311 6338
E-mail: kutilek@ecn.cz

2 SOIL POROUS SYSTEM

The term pore denotes that part of the soil space which is not filled by the soil solid phase The shape, size and origin of pores play a role only in a detailed classification of the soil porous system. Inasmuch as all transport processes and the storage of water occur in the soil porous system, we must study it in detail

2.1 SOIL POROSITY

The relative volume of pores is denoted as soil porosity

$$P = V_P / V_T \qquad (2.1)$$

where V_p is the volume of pores and V_T the total bulk volume of soil When (2.1) is multiplied by 100, we obtain P in percent The volume of pores V_P is related to the volume of soil solid phase V_S by the void ratio

$$e = V_P / V_S \qquad (2.2)$$

with mutual relations between P and e being

$$P = \frac{e}{1+e} \qquad \text{and} \qquad e = \frac{P}{1-P} \qquad (2.3)$$

Void ratio is more appropriate than porosity if the reference term V_T is not constant as for example in clays when they swell or shrink

Estimating the proper size of V_T is crucial It may be obtained by the following theoretical treatment, see Fig 2.1 Let us assume that when V_T is small enough ($V_T < V_P$) and centered in a pore, $P = 1$ When V_T is centered in the solid phase and small enough ($V_T < V_S$), $P = 0$ When V_T increases, we reach the situation when either $V_T = (V_P + \delta V_S)$ or $V_T = (V_S + \delta V_P)$ and porosity is neither 1 nor 0 Centering V_T in the solid phase, P is slightly above zero With a gradual increase in V_T we obtain first a gradual decrease of P (center in the pore) or a gradual increase of P (center in the solid phase), until both values coincide Before coincidence occurs, a damping oscillation of P may exist At this stage of increasing V_T when porosity is independent upon the initial centering of V_T, we have reached the representative elementary volume REV (Bear, 1969 and 1972) This final volume V_T is called by Corey (1977) the minimum volume of a reference element If V_T = REV, translating the center of V_T does not change the value of P The concept of REV is important in methods of practical determination of porosity as well as the application of the theory of potential flow to the description of water flow in soils Soils without structural development have an REV of about 100 cm^3 or less Because the REV of aggregated soils depends upon the size and shape of their peds, its value may be one or more orders of magnitude greater

Soil porosity manifests a broad range of values from less than 0.3 to more than 0.9 However, in the majority of mineral soils, P lies between 0.4 and 0.6 Some organic soils have values of P that exceed 0.9. Porosity depends upon the composition, texture and structure of soil Soil structure is influenced by the content of organic matter, the quantity of inorganic cementing agents, the genesis of the soil and its horizons and more recently, by human activity

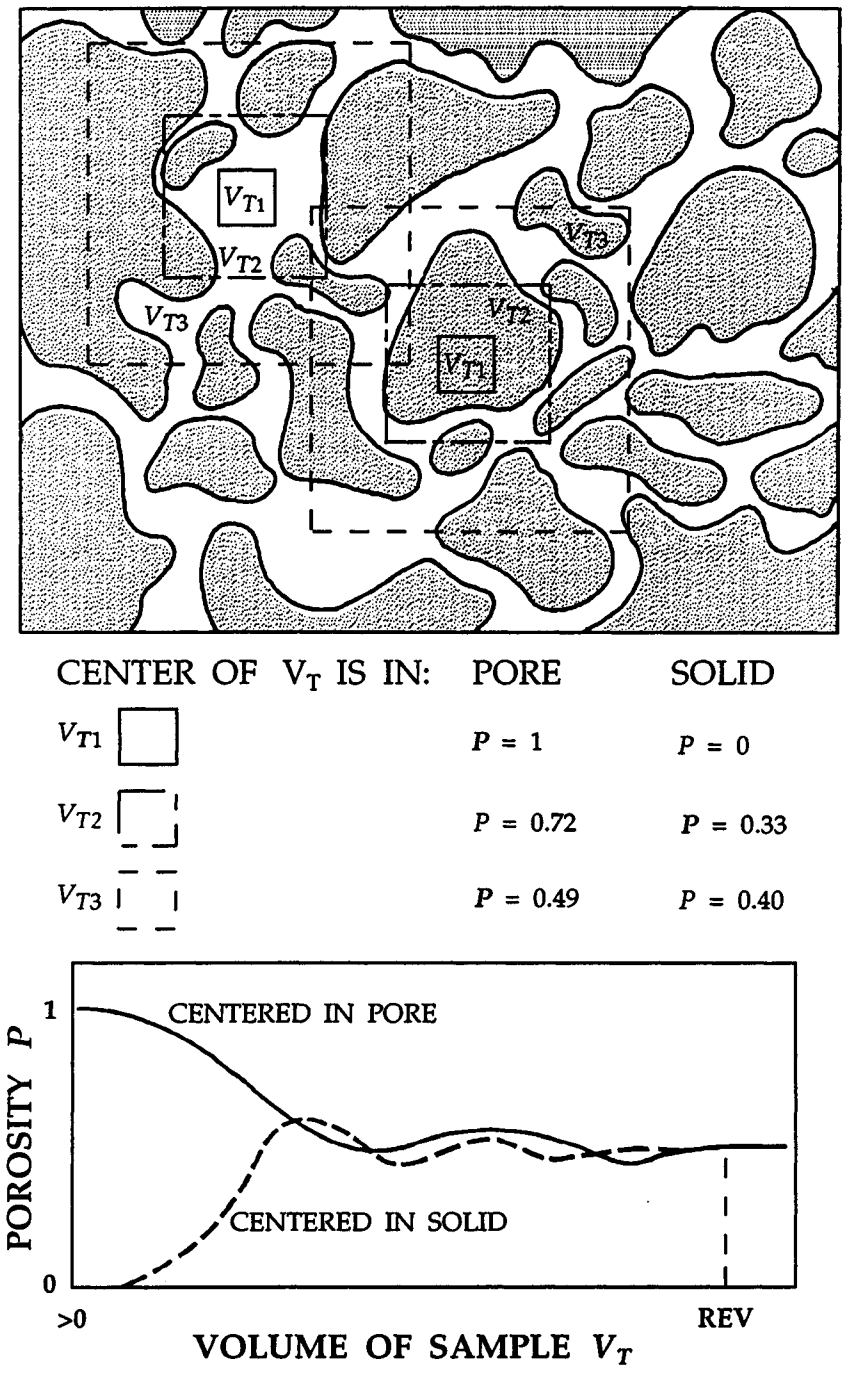

Figure 2.1. Estimation of Representative Elementary Volume REV by increasing the bulk volume of soil V_T to such an extent that porosity is independent of the position of the center of V_T.

Theoretically, in the most dense arrangement of spherical particles of identical size, $P = 0.26$. Although this value is sometimes taken as the theoretical minimum porosity of sands, even sandy soils are mixtures of particles of various sizes and shapes. Hartge (1978) reviewed binary and ternary mixtures of particles having different sizes and shapes. Even in the case of sands, neither simple nor sophisticated geometric models of the arrangement of particles are applicable for use of porosity.

With an increase of clay content the porosity of soils rises, owing mainly to a greater opportunity for soil aggregation. For soils not intensively cultivated, the mean values of porosity in the A-horizon and sub soil are plotted versus texture in Fig. 2.2. The porosity of the A-horizon reaches its maximum value in loamy soils owing to the optimum conditions for aggregation. In clays, the tendency to slushiness leads to a slight decrease of P. The data for the graph stem from research performed 70 years ago by Janota (1924) and were summarized by Kutílek (1978). The use of heavy machinery, the application of fertilizers in high quantities and the decrease of organic matter in soils – all specific features of modern-day intensive agriculture – decrease aggregation and enhance soil compaction. Hence, the porosity of most agricultural soils no longer depends upon soil texture.

The range of values of porosity found in four major textural categories of mineral soils according to Schachtschabel et al. (1984) is given in Table 2.1. Except for clay soils, texture does not significantly influence porosity. In clay soils originating from volcanic ash which are classified as Andosols, porosity reaches extreme values of 0.7 to 0.8.

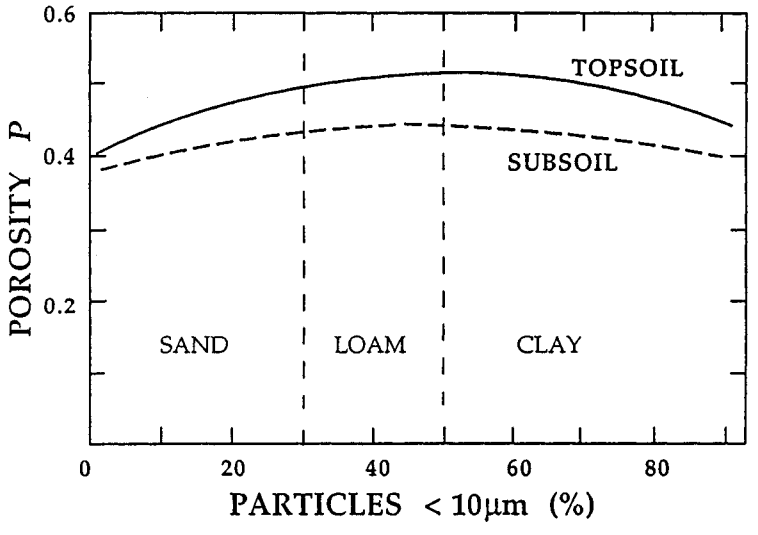

Figure 2.2. Dependence of porosity P upon the texture of the topsoil and subsoil of central European soils at the start of this century (Janota, 1924, and Kutílek, 1978).

Table 2.1. Range of the porosity and bulk density in mineral soils with $C_{ox} \leq 2\%$ (Schachtschabel et al., 1984).

Type of soil	Porosity P	Bulk density ρ_T
	%	$g \cdot cm^{-3}$
sandy soils	56 - 36	1.16 - 1.70
silty soils	56 - 39	1.26 - 1.61
loamy soils	55 - 30	1.20 - 1.85
clayey soils	70 - 35	0.88 - 1.72

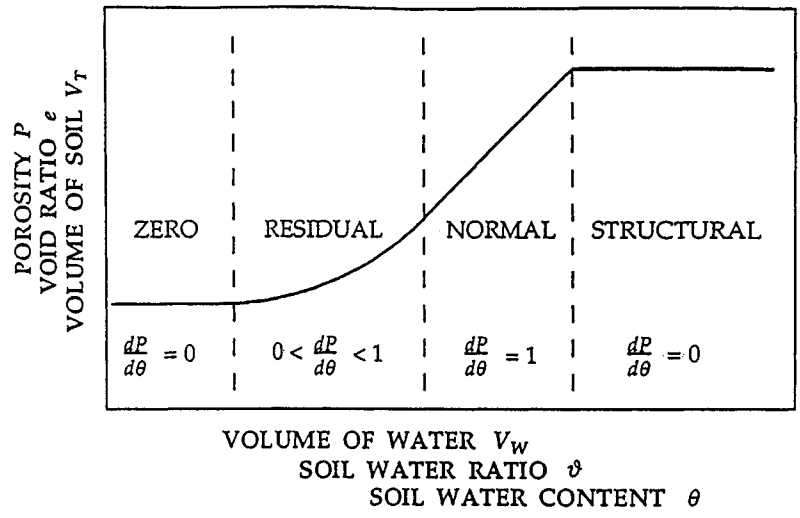

Figure 2.3. Dependence of porosity P upon soil water content θ in swelling soils. Four domains are defined (Haines, 1923, and modified by Yule and Ritchie, 1980).

In some clays and loams, P depends upon the soil water content θ inasmuch as soil swells when wetted and shrinks when dried. In such soils P increases with θ as shown in Fig. 2.3. This relationship is linear for large values of θ. At smaller values of θ, P changes non-linearly with θ. A detailed discussion is in section 3.1.

In the soil profile, the maximum porosity usually occurs in the top of the A_0 horizon. The porosity distribution with soil depth depends upon the development of each soil profile. For example, in the illuvial Bt horizon

accumulated material causes a decrease in porosity. Or, the reduction of iron oxides and the destruction of the structure in hydromorphic gley G horizons lead to an abrupt decrease in porosity.

The porosity of organic soils is greater than that of mineral soils and reaches maximal values in highly decomposed low moor. As mineral substances increase in organic soils the porosity decreases.

2.2 CLASSIFICATION OF PORES

2.2.1. Hydrologic Classification

According to Corey (1977), the classification of soil pores should follow the laws of hydrostatics and hydrodynamics and leads to main three categories, which are further subdivided (Kutílek and Nielsen, 1994):

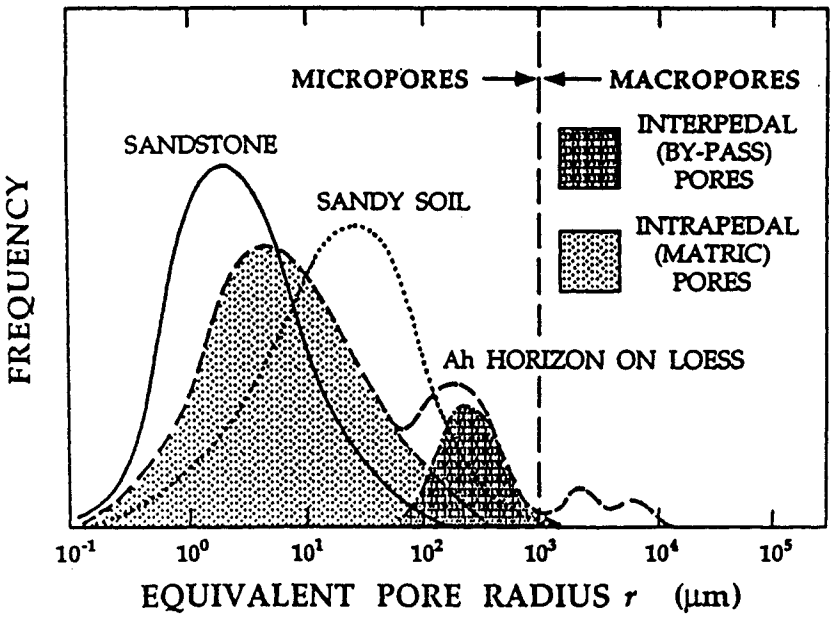

Figure 2.4. Schematic example of pore size distribution in parent rock and in soils.

1. Submicroscopic pores, which are so small that they preclude clusters of water molecules to form fluid particles or continuous flow paths. Inasmuch as convention does not exist in these pores, the laws of fluid mechanics are not applicable. Pores belonging to this category are oftentimes neglected.
2. Micropores or capillary pores. Transport processes in bodies with microporous systems are described by Richards' eq. and by convective-diffusion eq. We distinguish:

2.1 Matrix (intrapedal) pores within soil aggregates, their shape, size, coatings of walls, cuttans and nodules depend upon the soil genesis and they are stable in long term time span if no amendments are applied.

2.2 Interaggregate (interpedal) pores between the soil aggregates. They are stable in soils which are not affected by intensive agriculture with heavy machinery and high application of fertilizers, and their morphology depends upon the soil genesis. In soils under intensive agriculture their volume and shape are negatively influenced. The boundary between the two categories has to be defined from the analysis of pore size distribution, the equivalent pore radius is with rough approximation between 15 to 30 μm. Interaggregate pores are sometimes misinterpreted as macropores.

3. Macropores, or non-capillary pores of such a size that capillary menisci are not formed across the pore, the shape of air-water interface is planar. The boundary between micropores and macropores is formed by the equivalent pore radius approximately r = 1 to 2 mm. The flow of water inside of these pores is either in the form of a film on the walls of the pore, or filling the whole crossectional area of the pore, described either by a modified form of the Chézy eq., or by the kinematic wave eq. Origin of macropores is closely correlated to their stability and persistence in time:

3.1 Macropores formed by the activity of pedo-edaphon as decayed roots, earthworm channels etc. They have tubular form and they are well persistent in time and relatively independent upon variation of the soil water content. Some channels originated from the hair-roots may belong to the category 2.2 of micropores.

3.2 Fissures and cracks occurring as the consequence of volumetric changes of swelling-shrinking soils. They have planar forms and they are dependent upon the soil water content, at their high values they gradually disappear.

3.3 Macropores originating due to the soil tillage. Their depth is limited, they are dependent upon soil water content and disappear usually in less than one vegetation season, the persistence depends upon meteorological situations and type of plants.

Soil porous system with 2.1. plus 2.2. is sometimes denoted as system with dual porosity. In some instance soils with micropores and macropores are denoted as soils with dual porosity. The terminology is not unified. The same is for the quantitative characteristic of macropores.

Although the relative volume of macropores, category 3, is very small, it may have great impact relative to flows of water and its dissolved constituents within a soil profile.

2.2.2. Agronomic Classification

In soil science applied to practical agronomy, drainage and irrigation, capillary pores (in the second category) are frequently subdivided according to practical aspects of agriculture. Pores containing water below the permanent wilting point of plants are designed as fine pores, those with water between the wilting point and field capacity are medium pores and those with water above field capacity are coarse pores. The system is loose and without more specified definition of boundaries could result in misunderstanding. I am not recommending its use.

In soil science, two terms are used to describe soil porosity – primary porosity and secondary porosity. Primary porosity denotes the relative volume of pores owing to the shape and size of primary particles. Secondary porosity denotes the action of other factors, e.g. tubular pores form after the decay of plant roots, or fissures develop as the result of drying of soils that swell and shrink. Hence, Katchinski (1965) defines aggregate porosity P_A and interaggregate porosity P_B in terms of the average porosity of the individual aggregates $\overline{P_I}$ as

$$P_A = \frac{\overline{P_I}(1-P)}{1-\overline{P_I}} \qquad (2.4)$$

and

$$P_B = P - P_A, \qquad (2.5)$$

respectively. The terms intrapedal pores and interpedal pores are sometimes used for P_A and P_B, respectively.

2.2.3. Morphologic (or soil science) classification

The system was originally proposed by Brewer (1964) who was dealing mainly with soil micromorphology. His pore size classification is frequently used and we find it in Glossary of Soil Science Terms, 1996 (SSSA, 1997)

Class	Subclass	Class limits Equivalent diameter, mm	Pressure head - cm
Macropores	Coarse	>5	>0.6
	Medium	2-5	0.6-1.5
	Fine	1-2	1.5-3
	Very Fine	0.075-1	3-40
Mesopores		0.03-0.075	40-100
Micropores		0.005-0.03	100-600
Ultramicro-pores		0.0001-0.005	600–30000
Cryptopores		<0.1	<30000

2.3. MODELS OF SOIL POROUS SYSTEMS

The development of models is characteristic by the gradual transition from the simplest concepts up to the sophisticated approaches which are assumed to represent the complicated reality of soil pores. Thus, we can follow the process of successive improvement of models.

2.3.1. Assembly of spheres

Soil is modeled as an assembly of spherical particles. The volume of space between the spheres represents the porosity in unit volume of spheres. In the first models, the spheres were arranged either in a cubic or in a hexagonal net, Fig. 2.5. If the diameter of spheres is uniform we obtain porosity P = 47.64 % for the cubic arrangement and P = 25.95 % for hexagonal arrangement. The first type of assembly is the extremely loose one, the second one is the maximum dens one for uniform cubes.

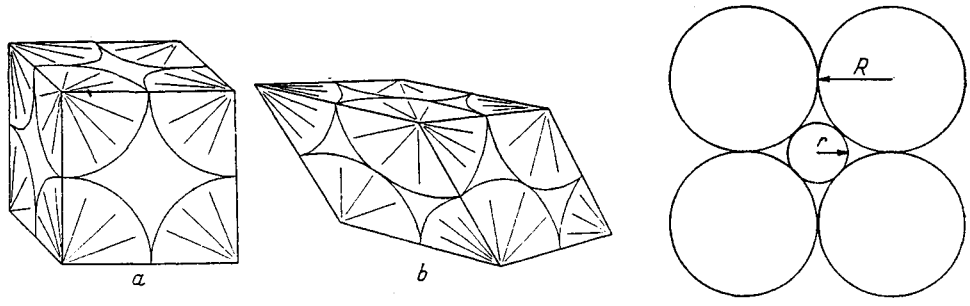

Figure 2.5. Model consisting of spherical particles in a) cubical, b) hexagonal arrangement.

This model is the oldest one in soil-water studies. The first authors using it for the study of soil capillarity were Keen (1924), Fisher (1924) and Haines (1925). We find it even in some of the recent studies (Iwata et al., 1988). The model of equal diameter of spheres was further completed by the assumption on existence of spheres of variable diameter. The particle-size distribution was considered as reference.

Arya and Paris (1981) assumed that the similarity between the shapes of the particle size distribution curve and the soil water retention curve SWRC is closely related to the value of the representative pore diameter in each of the defined particle size classes. The main disadvantage of models based upon similarity of spheres and soil particles is the negligence of the internal architecture of soil. The porous system of soil is formed by a certain configuration of particles into aggregates and the aggregates further being arranged in a definite way. However, when the particle-size distribution of a soil is determined, the aggregates are destroyed and individual particles separated. The particle-size distribution is a sort of an artefact. These models therefore approximate roughly the relations in sands only.

2.3.2. Parallel Capillary Tubes

The simplest model is the arrangement of **capillary tubes of equal diameter in a parallel way**. It was applied in soil and groundwater hydraulics by Kozeny in 1927 for the first time. The model is implicitly used even in some recent models of saturated hydraulic conductivity K_S . In order to get the model closer to the reality of the soil porous system with pores of various shapes and with curvature of the flow paths on microscale, the tortuosity factor was introduced by Kozeny.

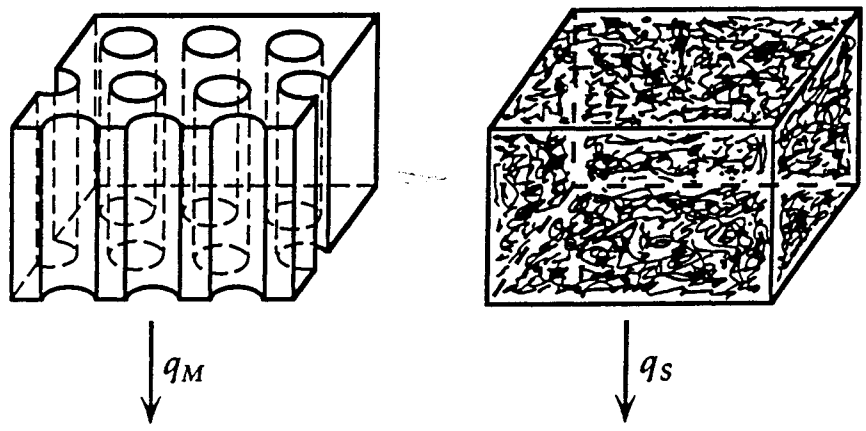

Figure 2.6

In Kozeny's model, the complicated soil porous system (right) is represented by a bundle of parallel capillary tubes of uniform radius (left). The flux density q, saturated hydraulic conductivity K_S, porosity P and surface area of pores A_m are the same in both the model and the soil.

From those equalities we obtain the radii of capillaries and the number of capillaries in the unit volume.

The Kozeny's model is not useful either for modeling of the soil water retention curve SWRC, or for explanation of the unsaturated hydraulic conductivity function *K(h)*, see unsaturated flow.

A simple model of a **bundle of parallel capillaries of non constant radii** was therefore applied for physical interpretation of SWRC (Figure 2.7.) and unsaturated hydraulic conductivity function (Childs and Collis George, 1950). A refinement of this model considers the capillaries as being rosary (ink-bottle) tubes. This allows hysteresis of SWRC, existence of entrapped air when the dry system is wetted etc.

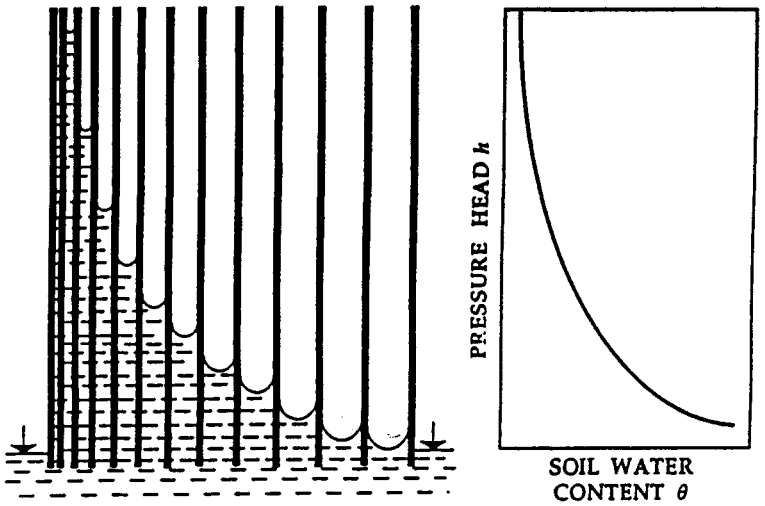

Figure 2.7 *Model of SWRC consisting of parallel capillary tubes (left) and the resulting SWRC (right).*

When the scale of the soil water pressure head on the axis of the SWRC is replaced by that of the radius of the capillaries according to (4.11), we obtain the summation curve of the pore size distribution. The derivative of this summation curve is the frequency curve of the pore size distribution, see Fig. 2.4. The frequency curve is advantageously expressed by equations of probability density functions (Brutsaert, 1966). Among the more common functions are the incomplete gamma distribution, the log-normal distribution and the first asymptotic distribution. Criteria for optimal selection of the applied probability density function are the same as those used in ordinary statistics, e.g. the χ^2 test or Kolgomorov-Smirnov test. A frequency curve can be used to discuss the quality of the soil pore space and the influence of society's activity upon its alteration.

Soil water retention curves SWRC plotted according to equation either of van Genuchten, or of Brooks and Corey are in Fig. 2.8 with θ soil water content and h the pressure head. Equivalent pore radius $r = 0.15\ h$ is plotted on the horizontal axis below pressure head h. The curves are thus summation curves of pore size distribution as well, provided that the parallel capillary tube model is applied. The derivation curves are plotted in the figure, too. They represent pore size distribution curves.

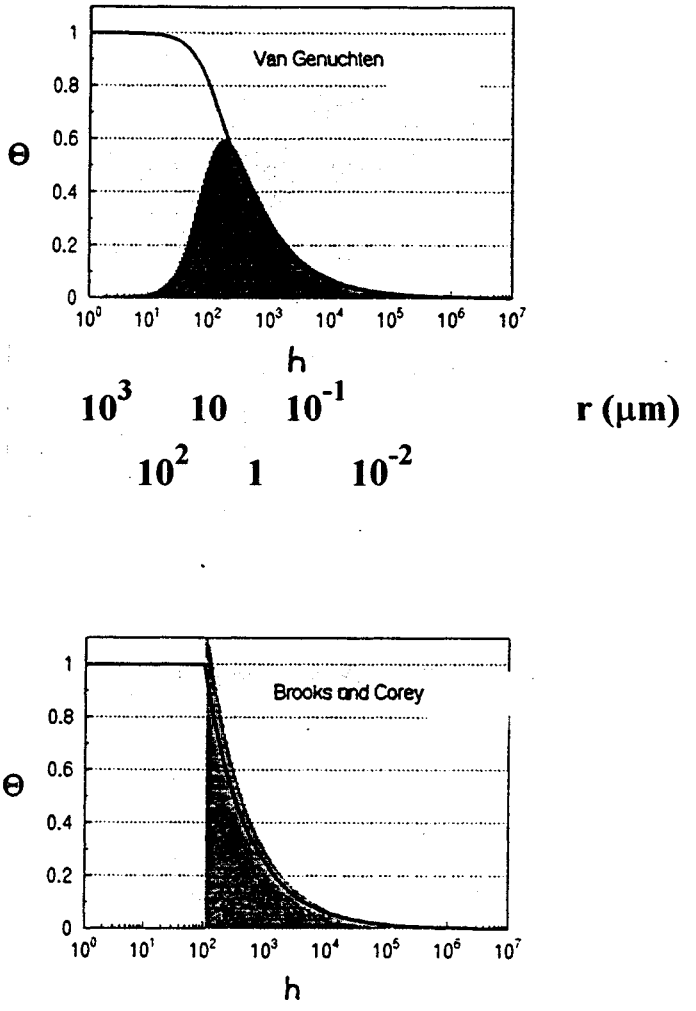

Figure 2.8. Pore size distribution in SWRC models of van Genuchten and Brooks and Corey

SWRC has frequently more than one inflection point. We find therefore more than one peak in pore size distribution curve. In Fig. 2.9 is the example of a bi-modal distribution curve as typical for soils which have two categories of capillary pores according to hydrologic classification: Matrix (intrapedal) pores, Class 2.1 and interaggregate (interpedal) pores, Class 2.2.

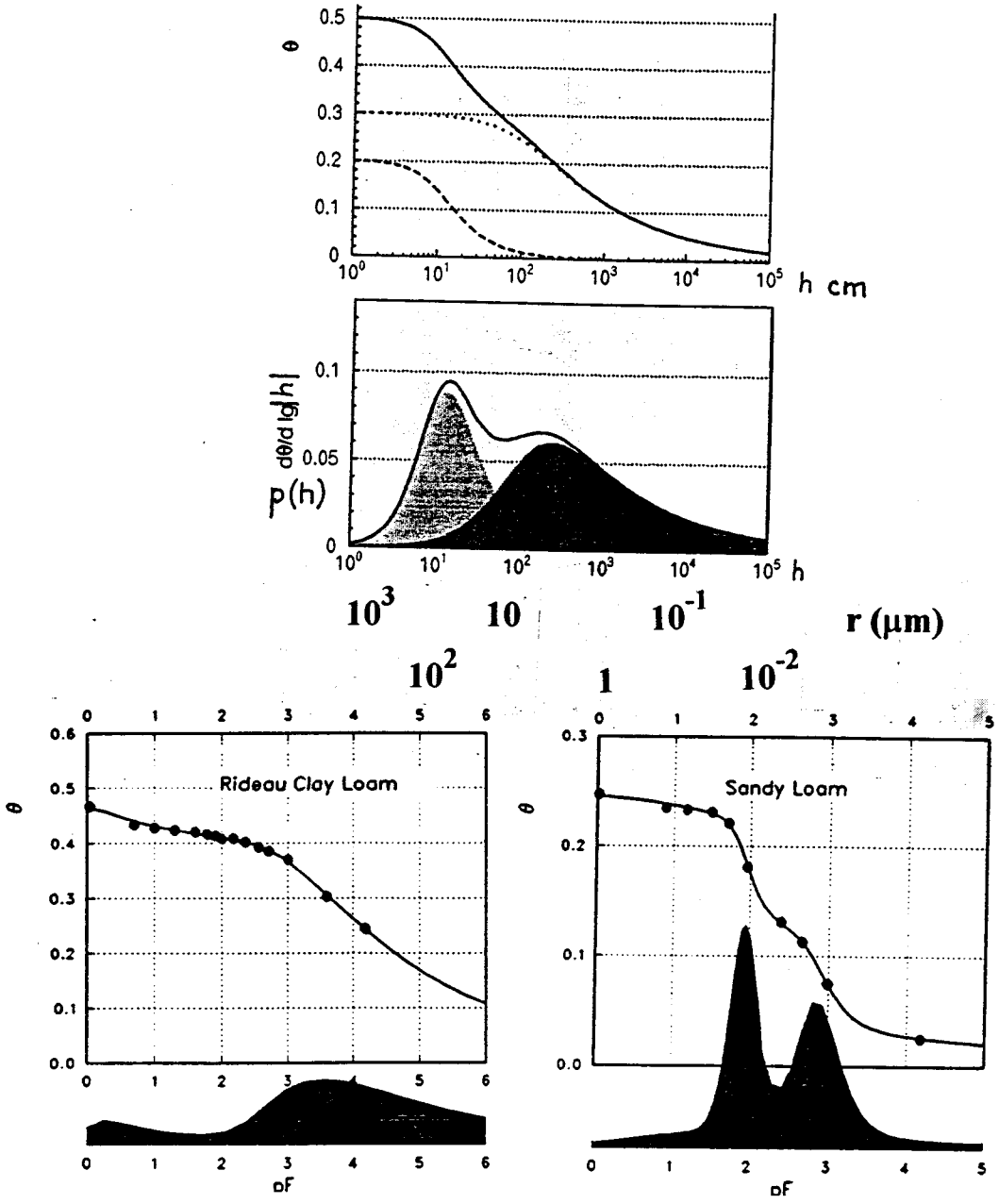

Figure 2.9. Bi-modal pore size distribution (Durner, 1991, 1992)

Bi-modal (or dual) system of capillary pores is usually well developped in A-horizon, and less in B and C-horizons of soils. Generally, bi-modality is decreasing with the depth (Othmer et al., 1991).

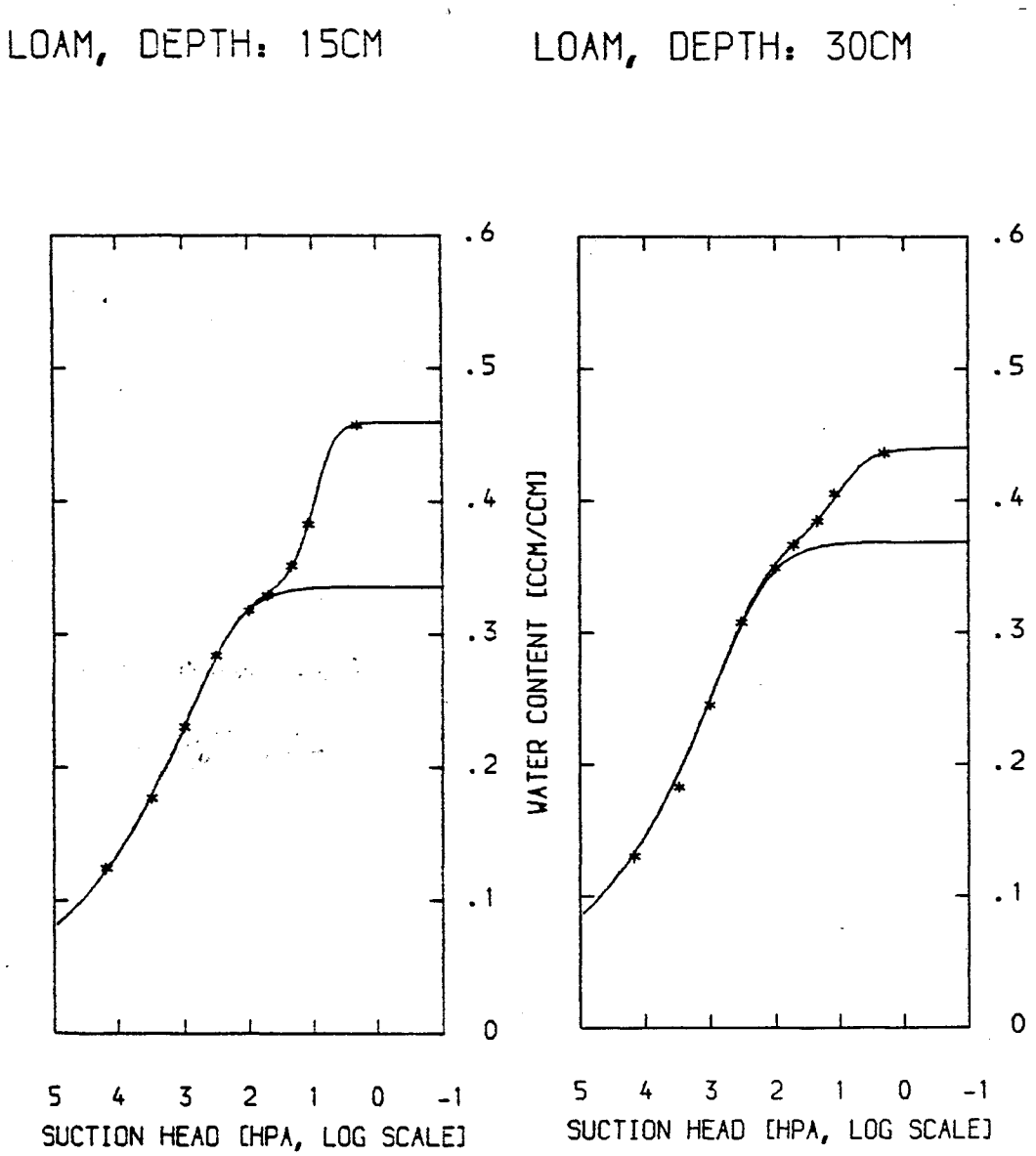

Figure 2.10 a. SWRC of a bi-modal porous system in A and A/B horizon of a Cambisol.

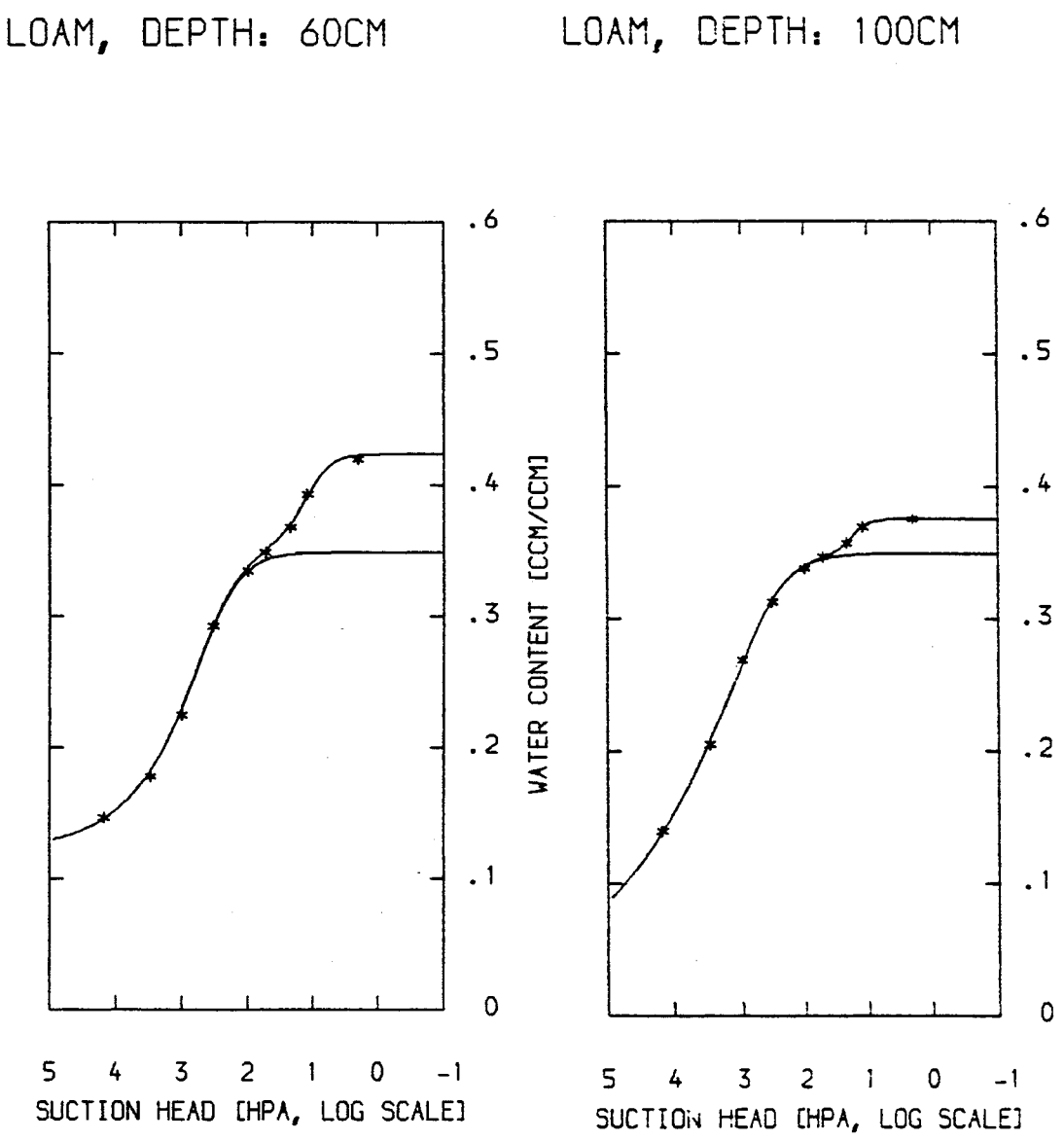

Figure 2.10 b. SWRC of a bi-modal porous systém in B and C horizons of a Cambisol.

2.3.3. Percolation models

Fatt (1956) was probably the first to realize that imperfections in parallel capillary models required a new approach to model porous media. He proposed an empirical, two-dimensional network of capillaries having randomly distributed radii. This lattice type network of pores was extended to a 3-dimensional network and for the solution of equilibria between the soil water potential and θ, percolation theory was applied (Chatzis and Dullien, 1977; Wardlaw et al., 1987; and Diaz et al., 1987). With the soil water potential being identified with the capillary potential, the model was hypothetically placed into the pressure apparatus. We shall first use the simplest type of percolation model which is a 2-dimensional square network where the pores are represented by mutually interconnected perpendicular cylindrical tubes of various radii. The radii are scattered randomly in the network with a prescribed distribution function $\rho(r)$. Inasmuch as the number of segments n approaches infinity in percolation theory, models of the theory usually contain segments $n > 1000$. Here for the sake of clarity in Fig. 4.20, we use only 72 segments.

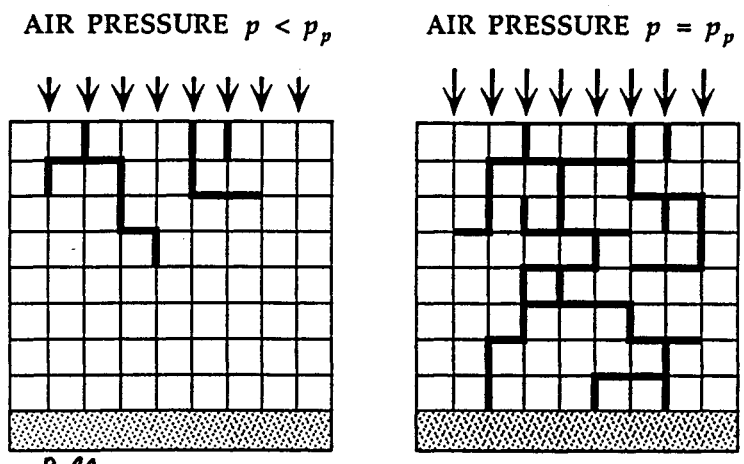

2.11

Figure 4.20. Pre-percolation (left) and percolation stage (right) in a 2-dimensional model consisting of capillary tubes of randomly distributed radii. Thick lines denote capillary tubes filled with air when the model is placed in a pressure plate apparatus.

This 2-dimensional model is conceptually first completely saturated with water and placed in a pressure plate apparatus. Similar to the method described in section 4.3.1, the air pressure is gradually and incrementally increased. When

the pressure head h is below the percolation threshold $|h| < h_p$, water is replaced only in a very small portion of pores of radii r defined by (4.11) as

$$r \geq r_h = \frac{2\sigma \cos\gamma}{|h|\rho_W g}. \qquad (2.7) \quad \text{(4.45)}$$

The great majority of pores having radii $r \geq r_h$ is surrounded by pores having radii of $r < r_h$. At this small initial value of pressure head h, the cluster of air-filled pores close to the top surface of the model is negligible and the model is not effectively drained. When the air pressure in the apparatus reaches the percolation threshold h_p, water is replaced by air in a continuous cluster of pores, all of radii $r \geq r_{hp}$, see Fig. 4.20. Isolated groups of water-filled connections of radii $r > r_{hp}$ remain undrained because they are surrounded by air-filled connections leaving them isolated and without a continuous path to the semipermeable membrane of the apparatus and to the free water pool. When the air pressure is further increased in our model, no additional drainage is realized and this is denoted as the post-percolation stage. A SWRC of such a model is step-like.

When the model still consisting of perpendicular capillary tubes is extended to a 3-dimensional net, drainage does not stop at one percolation stage but proceeds further when the external pressure is increased. The SWRC of the 3-dimensional net does not yield a unique step-like form similar to that of the 2-dimensional model. Owing to the three dimensionality of the net, clusters of undrained pores change and alter their configuration with a portion of undrained water remaining. Similarly, when water enters into a dry, air-filled model, clusters of pores remain filled with air in spite of the fact that they should be filled with water at the given pressure if water had free access to all pores. This procedure adequately explains the mechanistic part of hysteresis. With the occurrence of the clustering of entrapped water or air, the restrictive access of pore water or pore air to the outside pool of free water or free air is demonstrated.

Another type of 3-dimensional model consists of spherical pores interconnected by capillary tubes (throats). They are arranged in a cubical net, see Fig. 4.21. The throats may or may not be correlated to the spherical pores.

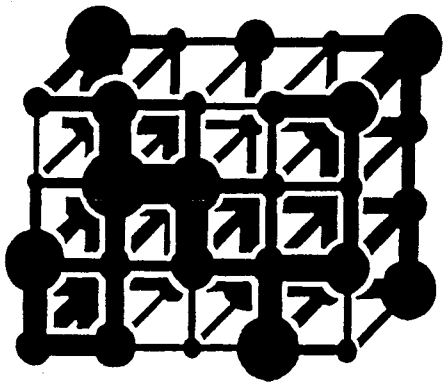

2.12

Figure 4.21. A 3-dimensional model consisting of spherical pores interconnected by capillary tubes (throats) whose radii are randomly distributed.

If we define the pore size distribution $\rho(r)$ in the cubic percolation lattice, demonstrated in detail in Fig. 2.14 b, we obtain SWRC related to this $\rho(r)$ pore size distribution, Fig. 2.13 a, b. The dotted curve in $h(\theta)$ graph can be interpreted as SWRC of a simple parallel capillary tube model, i.e. without percolation principles.

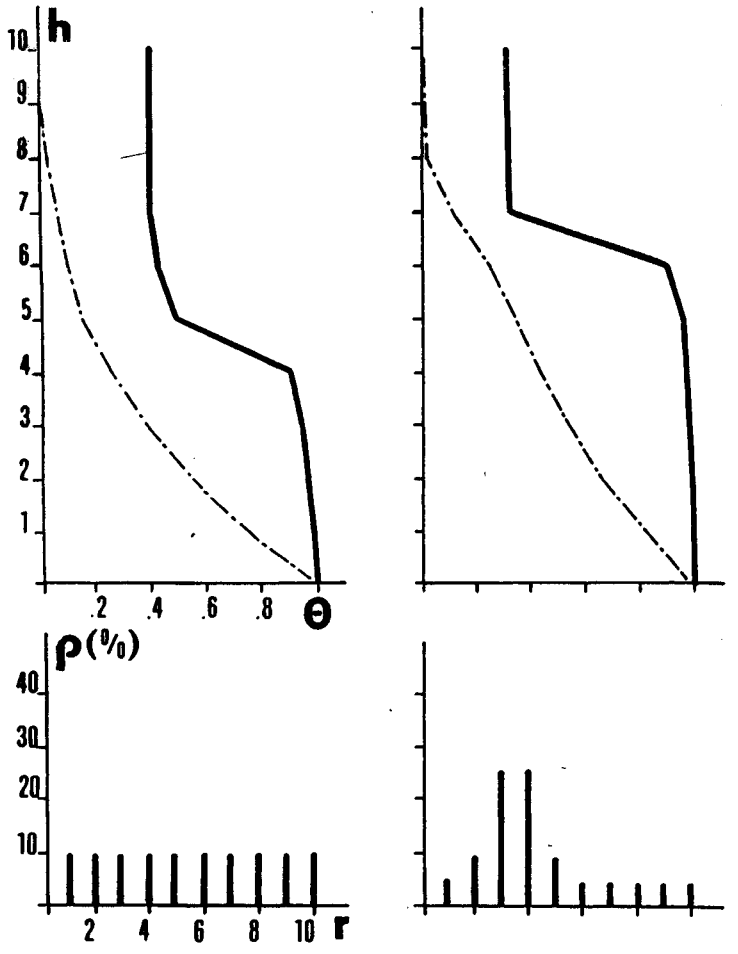

Figure 2.13 a. SWRC of a cubic percolation lattice with pore size distribution defined by $\rho(r)$.

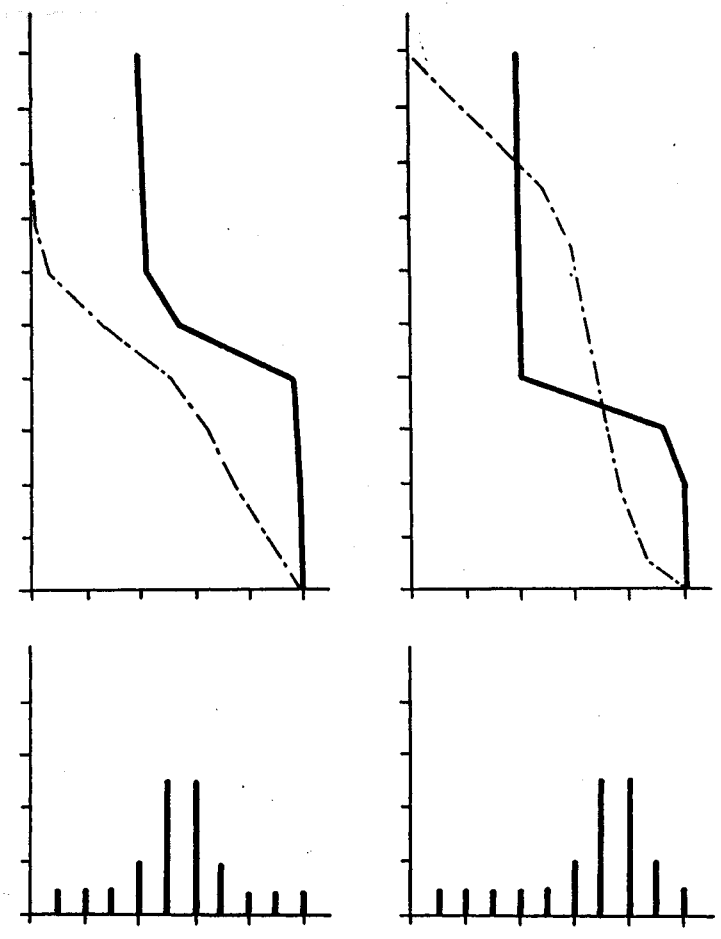

Figure 2.13 b. SWRC of a cubic percolation lattice with pore size distribution defined by $\rho(r)$, the parameters on the axis are the same as in Fig. 2.13 a.

A detailed review on percolation theory and network modeling as applied to soil physics is by Berkowitz and Ewing (1998). On next pages we reproduce their figures showing how the pore size models have been developed and what are the practical consequences of percolation modeling.

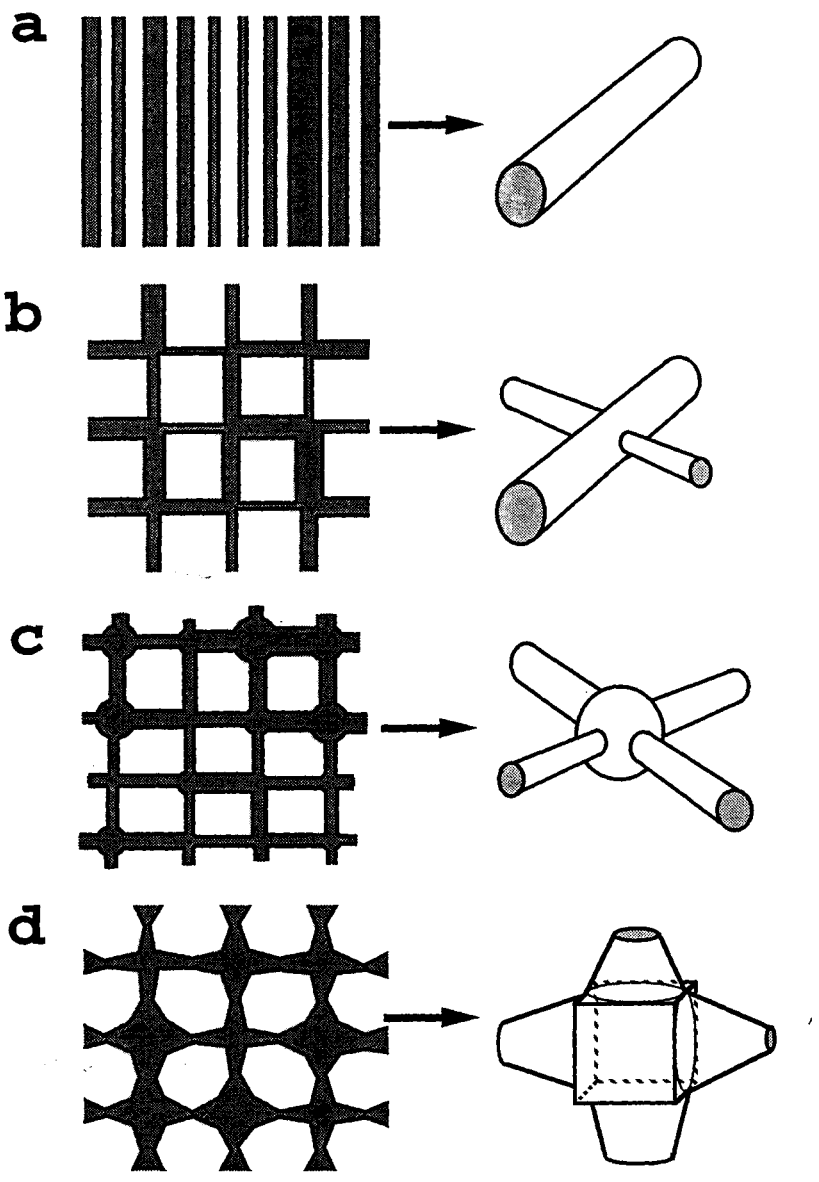

Figure 4. Evolution of pore space models. (a): parallel tubes, (b): tube network of Fatt (1956), (c): ball-and-stick network of Chandler et al. (1982) and Koplik (1982), (d): 2D version of Toledo et al.'s (1989) biconical pore network.

Figure 2.14

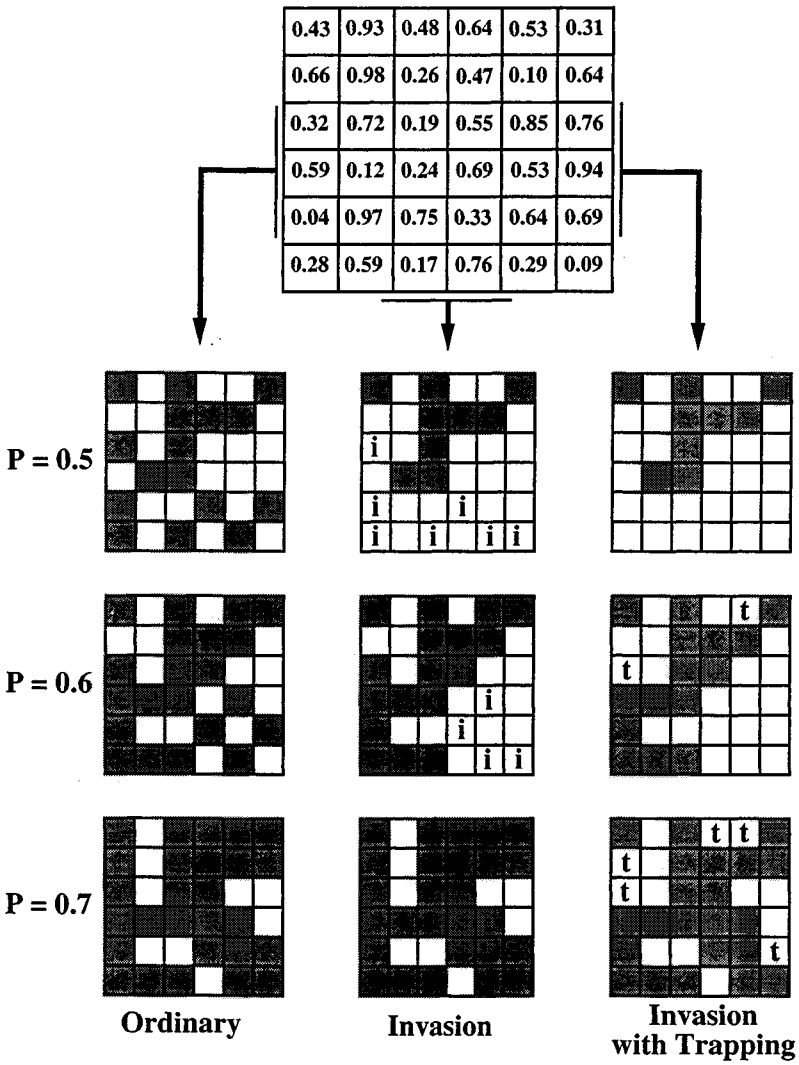

Figure 5. A comparison of ordinary percolation, invasion percolation, and invasion percolation with trapping. Invasion is from the top, and occupied sites are shaded. Numbers in the boxes at the top denote the invasion probabilities of the individual sites, while numbers down the side refer to the current occupation probability of the system. Sites marked with an "i" are invadable (sufficiently low probability) but inaccessible. Sites marked with a "t" are invadable and accessible, but trapped. As the occupation probability p increases, differences between ordinary and invasion percolation decrease, while differences between invasion percolation with and without trapping increase.

Figure 2.15

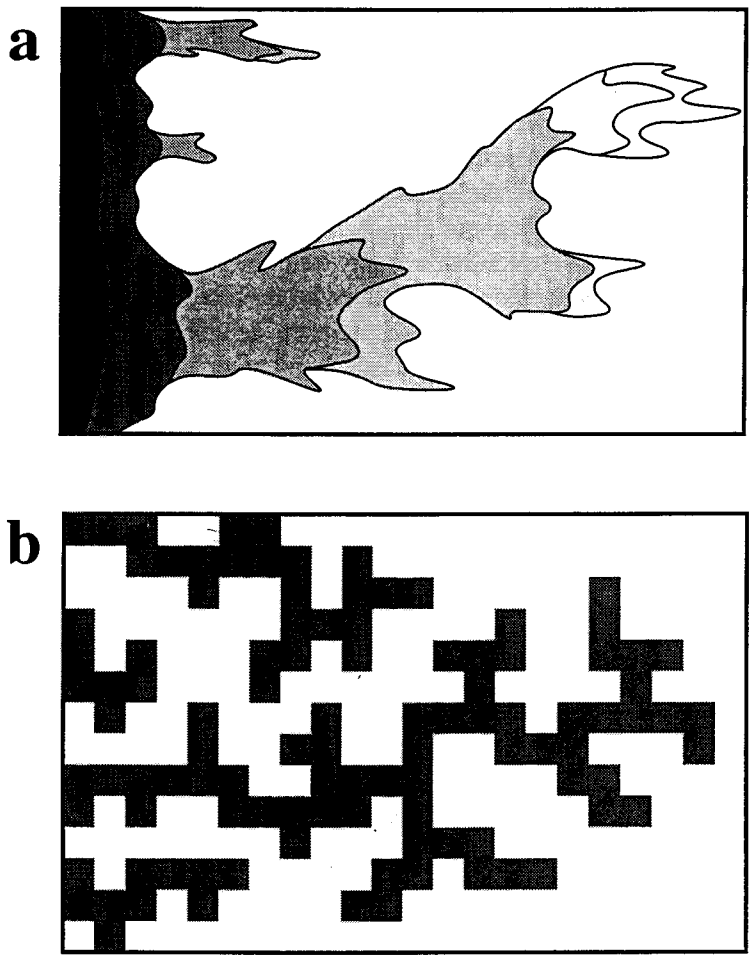

Figure 9. (a): Viscous fingering. Earlier times are shown with darker fluid. (b): Diffusion-limited aggregation (DLA), with the seed being the left side. In both cases, the interface moves from left to right.

Figure 2.16

Main disadvantage: If we want to use a percolation network model of a real soil and on a real soil, we have to know the pore size distribution, PSD. However, PSD from image analysis is 2-dimensional and not fully reliable for 3-dimensional models. PSD from mercury porosimetry is derived from bundle of parallel tubes. The same is for SWRC.

2.3.4. Fractal and Fractal Fragmentation Models

The term fractal is derived from the Latin word *fractus = fragmented, broken smashed.* It was introduced by the Polish born mathematician B. B. Mandelbrot in 1975 (quotation in Mandelbrot, 1982). Fractals are distinct from the simple objects of "classical" (Euclidean) geometry: The square, the circle, the sphere etc. They are capable of description many irregularly shaped objects that cannot be accomodated by Euclidean geometry. The concept of fractals deals with new system of geometry where the complex geometric shapes exhibit the property of self-similarity. A self-similar object is one whose components resemble the whole object. Reiteration of irregular details or patterns occurs at progressively smaller scales and can, in the case of purely abstract entities, continue indefinitely. Each part of each part, when magnified, will look like the object as a whole, see Fig. 2.18 and 2.19. i.e. a self-similar object remains invariant under changes of scale, it has a scaling symmetry, see later on the Miller-Miller (1956) concept of scaling of soil physical properties. If the number of iteration i has final value, the term prefractal is used, too.

Important characteristic of a fractal is the **fractal dimension.** It is generally expressed by a noninteger and it reveals precisely the nuances of the shape of a studied non-Euclidean figure. An example is in Fig. 2.17. The length of an irregular perimeter O is measured repeatedly by fixed measurement units of step length L, i.e. by stick of the length L. The shorter is this stick, the longer is the apparent perimeter O. L and O are related by the power law

$$O \propto L^{Dc-1} \tag{2.8}$$

Where D_c is the fractal dimension. It is related to the area A by

$$\alpha = \text{const.} = O^{1/Dc} / A^{1/2} \tag{2.9}$$

When this eq. (2.9) is rewritten in the logarithmic form, fractal dimension of the outline is found from the slope of log (O) on log (A). Single pore outlines are demonstrated in Fig. 2.17 (Pachepsky et al., 1996). **A circle will have $D_c = 1$.**

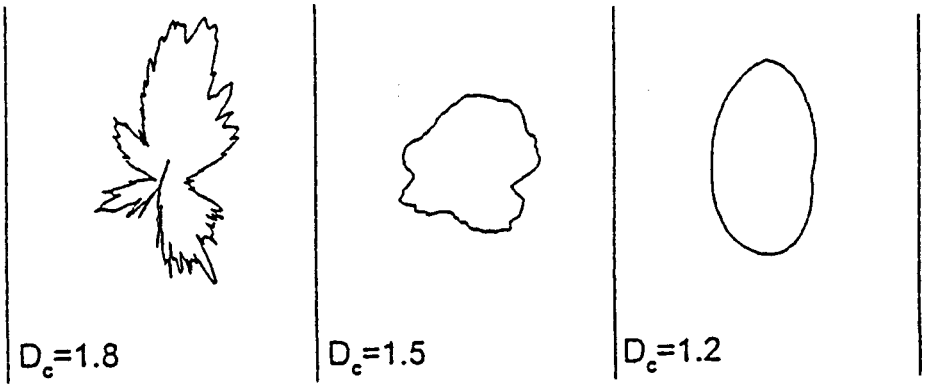

Figure 2.17. Single pore outlines with relevant fractal dimensions D_c

Simple deterministic fractals are constructed by repeating a pattern, named generator onto a starting object, named initiator. The initiator determines the dimensionality, while the generator defines the symmetry. The generator pattern is

repeated *i-th* times and can result either in accretion, or reduction of the initiator. In the Cantor bar, Fig. 2.18, the initiator is the solid line and the generator is the broken line. The number size relationship is

$$N(r) = kr^{-D} \tag{2.10}$$

Where $N(r)$ is the number of elements of length equal to r, k is the number initiator of unit length, further on $k = 1$ and D is the fractal dimension. From (2.10) in log form and after rearrangement is

$$D = \log[N(1/b^{i+1})/N(1/b^{i})]/\log(b) \tag{2.11}$$

For Cantor bar $N(1/b^{i+1})/N(1/b^{i}) = 2$, $b = 3$ and $D = 0.63$.
For Koch curve, Fig. 2.18 is $N(1/b^{i+1})/N(1/b^{i}) = 4$, $b = 3$ and $D = 1.26$.
For Sierpinski carpet, Fig. 2.18 is $N(1/b^{i+1})/N(1/b^{i}) = 8$, $b = 3$ and $D = 1.89$.
For Menger sponge, Fig. 2. 19 is $N(1/b^{i+1})/N(1/b^{i}) = 20$, $b = 3$ and $D = 2.73$.

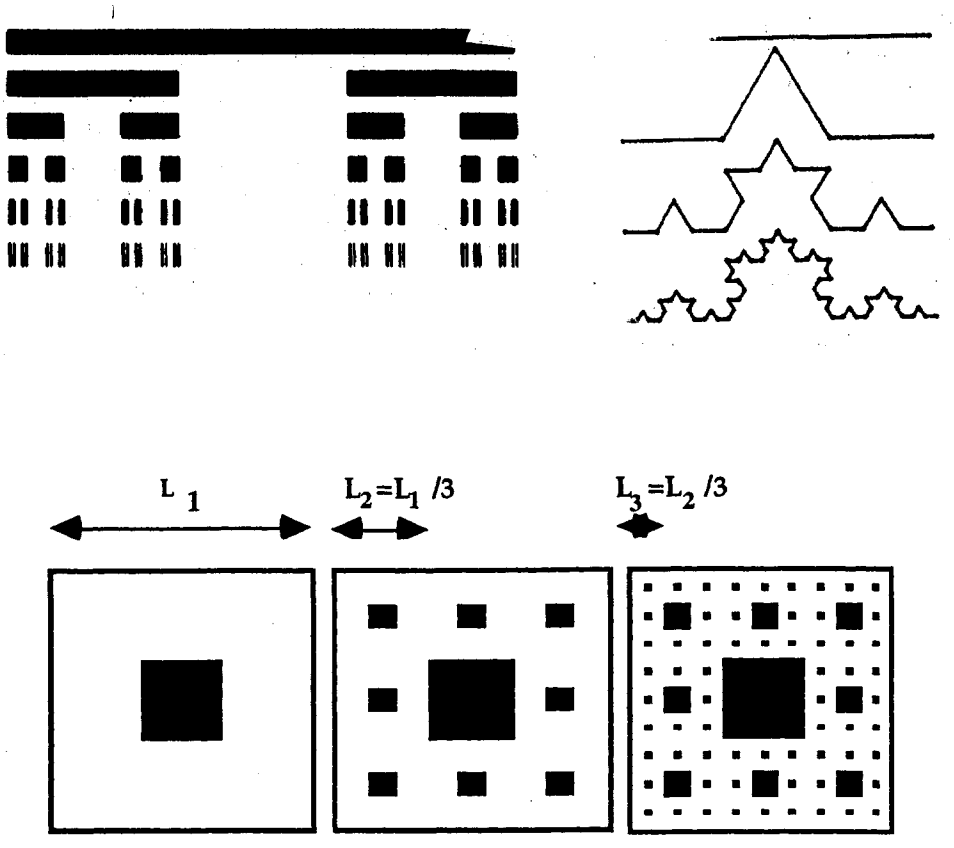

Figure 2.18. Deterministic fractals: Cantor bar (top left), Koch curve (top right) and Sierpinski carpet (bottom).

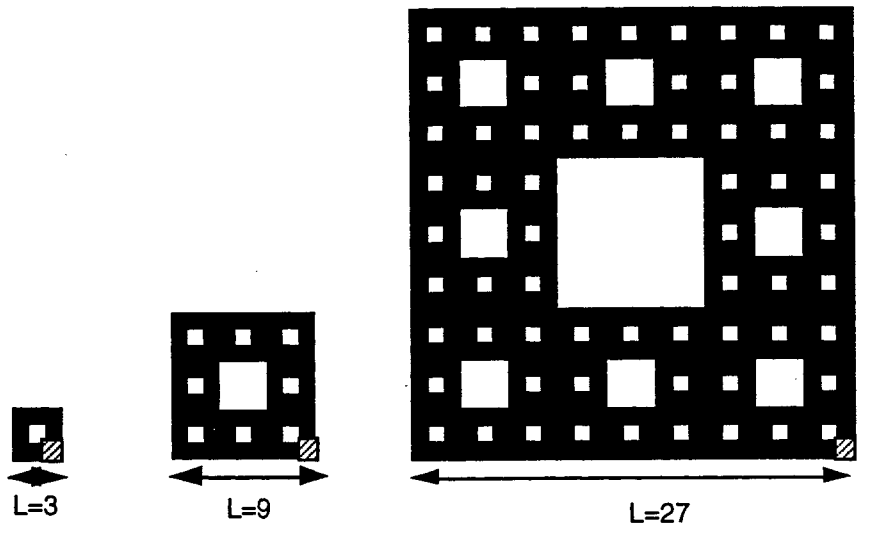

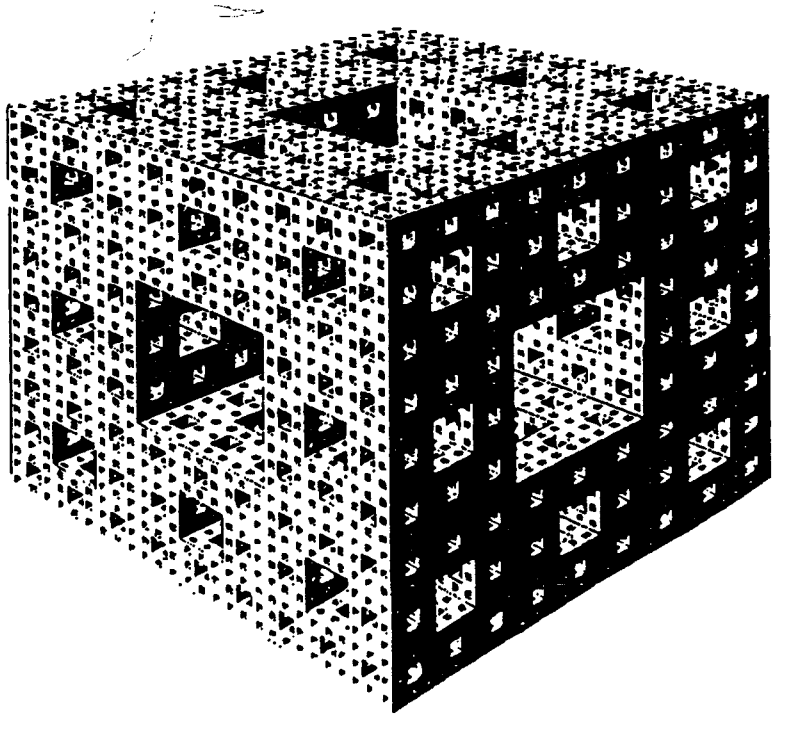

Figure 2.19. Reversed Sierpinski carpet (top). The area A(L) of the black (solid phase) is proportional to L^D. Menger sponge (bottom).

Several fractal dimensions can be used to characterize the geometry of a porous medium in relation to transport processes:

Fractal dimension of mass D_m describes space filling of the solid in a space of radius r

$$M \propto r^{Dm} \text{ with } D_m \leq d_T \quad (2.12)$$

where $d_T = 2$ for two-dimensional objects, $d_T = 3$ for three-dimensional space. It follows that there is a decrease of the density of fractal objects with increasing value of r. The value of D_m in $d_T = 3$ is usually between 2.75 to 2.95 in range of 10^{-1} to 10^{0} mm (Giménez et al., 1997).

Fractal dimension of pore volume D_v is obtained after development of the power law

$$V_p \propto r^{Dv} \text{ with } D_v \leq d_T \quad (2.13)$$

where $d_T = 2$ for a circle of radius r. The values of D_v are generally smaller and span a larger range than D_m values. D_v were found between 1.22 and 1.85 in majority of instances (Giménez et al., 1997).

Fractal dimension of pore surface D_s is governed by equation analogical to previous ones.. It is determined either by adsorption of water molecules, or from the intrusion of the non-wetting liquid (mercury). Large values of D_s are associated with increased percentage of clay minerals and with organic matter in soil, its small values are mainly related to inorganic "smooth" surfaces of sands.

Fractal fragmentation leads to a better understanding of relationships between aggregation, n-modal porosity and soil hydraulic properties. A scale invariant fragmentation process leads to a distribution of fragment sizes that follow the cumulative form of equation (2.10) where D is replaced by D_F.

Fragmentation starts with a set of initial points in a square P_0 , Fig. 2.20, top. Then a space partition is made in order to split P_0 into polygonal zones $P(M)$, each associated with point M (Voronoi tesselation, or Theissen polygon in hydrology), Fig. 2.20, bottom. Then a porous structure is created with $\underline{P}$ (G, k). G is the center of gravity, k is chosen to generate the given porosity. This process can be repeated on successive levels of fragmentation. What were earlier solid elements $P(M)$ are now aggregates that may be divided into smaller microaggregates or particles. The final fractal structure is defined by fractal dimension D_F. N polygons in 2-dimensions correspond to $\boldsymbol{n} = N^{3/2}$ in 3-dimensions, $\boldsymbol{r} = k/N^{1/2}$ in isotropic material and the fractal dimension is then $D_F = -\log \boldsymbol{n}/\log \boldsymbol{r}$. SWRC equation of Rieu and Sposito (1991) is

$$\theta(h) = (h/h_A)^{DF-3} + \theta_S - 1$$

Earlier expressions based on Brooks and Corey eq.

$$\theta(h)/\theta_S = (h/h_A)^{DF-3}$$

look as less appropriate, especially when we consider the empirical value of the exponent in Brooks and Corey eq. If percolation theory is applied for the description of the invading fluid into multi-level fragmented model, n-modal SWRC is obtained, including the hysteretic loop.

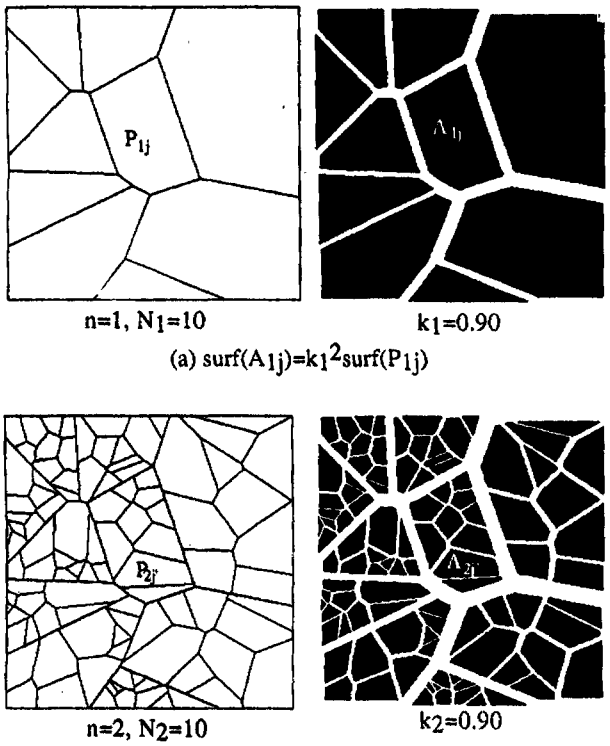

Figure 2.20. Construction of a soil structure on several levels of fragmenation, top: first level, bottom: second level (Perrier et al., 1955).

When the fractal fragmented model is applied to hydraulic functions and fluxes in soils, the percolation principles are applied for the interpretation of SWRC, hydraulic conductivity and dispersion in real soils with n-modal porosity.

Fractal dimension D may have different physical interpretation. Soil water retained in very small pores is likely to be a function of pore surface roughness and water retained in large pores is a function mainly of pore size. Therefore scaling of adsorption isotherms is mainly the function of pore roughness. Scaling of SWRC at low pressure heads is a function of both, pore size distribution and pore roughness, each characterized by its own value of fractal dimension. Scaling of SWRC at relatively high pressure heads is mainly a function of pore size distribution.

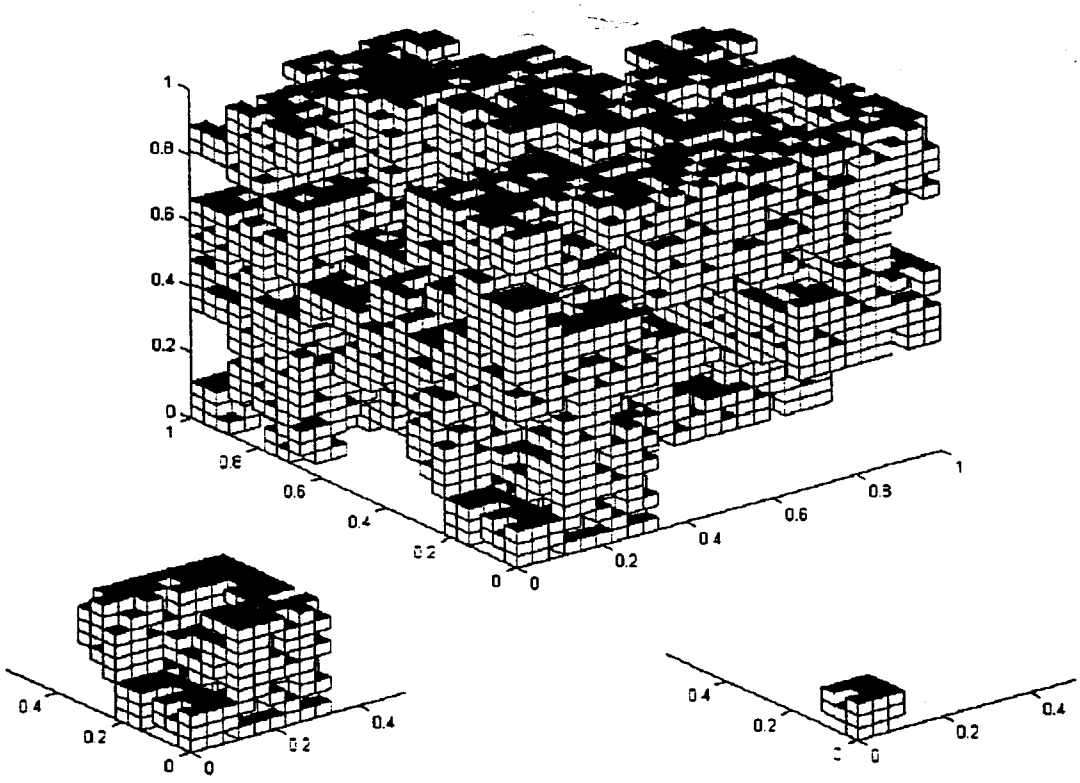

Figure 2.21. Fragments derived from a randomized Menger sponge (Perfect et al., 2001).